Electrostatically promoted dynamic hybridization of glucans with cationic polythiophene

Gaku Fukuhara, Mami Imai, Denis Fuentealba, Yuki Ishida, Hiroki Kurohara, Cheng Yang, Tadashi Mori, Hiroshi Uyama, Cornelia Bohne and Yoshihisa Inouea

August 2016 (online)

Organic & Biomolecular Chemistry

Accepted Manuscript

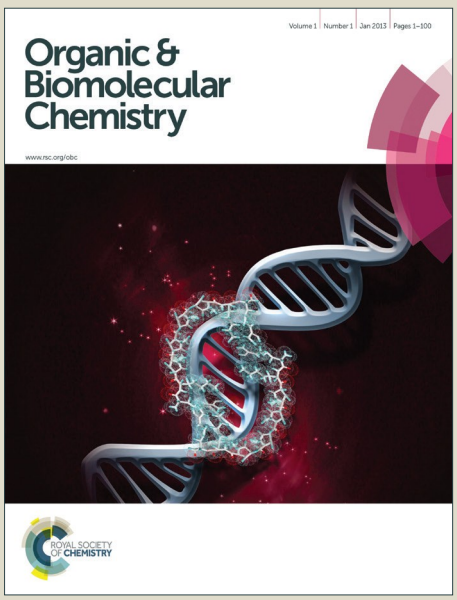

ROYAL SOCIETY OF CHEMISTRY

www.rsc.org/obc

Organic & Biomolecular Chemistry

PAPER

Electrostatically promoted dynamic hybridization of glucans with cationic polythiophene

Received 00th January 20xx,
Accepted 00th January 20xx

DOI: 10.1039/x0xx00000x

www.rsc.org/

Gaku Fukuhara,*[a] Mami Imai,[a] Denis Fuentealba,[bc] Yuki Ishida,[a] Hiroki Kurohara,[a] Cheng Yang,[ad] Tadashi Mori,[a] Hiroshi Uyama,[a] Cornelia Bohne[b] and Yoshihisa Inoue[a]

Hybridizing natural macromolecule with synthetic polymer is an efficient general method for constructing sophisticated supramolecular architectures. To comprehensively elucidate the controversial hybridization mechanism of glucans with synthetic polymers, the hybridization behaviors of triple-stranded curdlan (Cur) and schizophyllan (SPG) with cationic polythiophene (PyPT) were investigated in aqueous DMSO solutions by using UV-vis, circular dichroism (CD), fluorescence, fluorescence excitation, and NMR spectroscopies, as well as theoretical calculations, dynamic light scattering, and zeta potential measurements. Upon mixing with glucan, a hetero-triplex formed was dynamic and greatly accelerated by heating and by adding base or salt. The hetero-triplex disassembled to hetero-duplex in highly basic solutions. Thus, polycationic polymers, such as PyPT, are expected to serve as a versatile tool for unzipping glucan homo-triplexes and promoting subsequent hybridization in aqueous solution, while the detailed mechanism elucidated in the present study contributes to the rational design of hybridization partners.

Introduction

Inter-polymer interactions and polymer assemblies derived therefrom play essential roles in constructing natural and artificial supramolecular architectures. Of several approaches to novel functional polymer assemblies, hybridizing natural and synthetic polymers provides an efficient, promising strategy for merging the original structural features of natural polymers and the desired functions of synthetic polymers.[1] Nevertheless, the hybridization is not always feasible and the compatibility has to be examined on a trial and error basis. More crucially, changing hybridization partners often leads to different inter-polymer interactions and hence elucidating hybridization mechanisms and dynamics becomes the key issue. This ambivalence renders hybrid polymer research one of the most vital and challenging topics in current chemistry.[2]

β-1,3-Glucans are polysaccharides composed of (1→3)-linked β-D-glucose units with or without branching. Among them, curdlan (Cur) is the simplest in structure, possessing a linear main chain and essentially no branching glucose, while schizophyllan (SPG) has a glucose sidechain at every third glucose unit on the main chain (Fig. 1). This structural difference makes the former insoluble in water but the latter moderately soluble.[3,4] From the supramolecular viewpoint, one of the most intriguing features of Cur and SPG is their ability to reversibly denature (to random coil) and renature (to triple helix) by simply changing solvent from DMSO or aqueous alkaline solution to water or aqueous acidic solution.[3,4] Utilizing the reversible helix formation, Shinkai et al. demonstrated that water-soluble polythiophenes (PTs) form divergent complexes with triple-stranded SPG.[4,5] They also revealed that 6-*O*-modified Cur forms a complex with cationic PT in aqueous solutions,[6] but similar behavior has not been reported for native Cur. Two distinct mechanisms have hitherto been proposed for the hybridization of glucans with PT derivatives: (1) encapsulation of PT in the hollow core of glucan helix[5a,d,e,6b] and (2) cohelical complexation of PT with SPG duplex (to form hetero-triplex)[5f] or modified Cur single strand (to form hetero-duplex),[6a] both of which sound plausible and further mechanistic investigations are obviously needed.

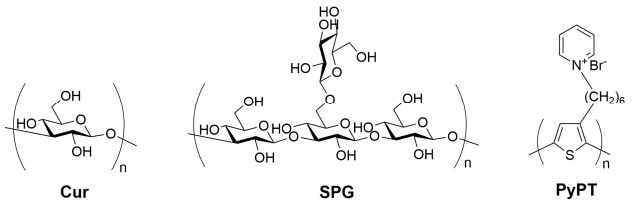

Fig. 1 Chemical structures of curdlan (Cur), schizophyllan (SPG), and pyridiniopolythiophene (PyPT).

[a] Department of Applied Chemistry, Osaka University, 2-1 Yamada-oka, Suita 565-0871, Japan. E-mail: gaku@chem.eng.osaka-u.ac.jp
[b] Department of Chemistry, University of Victoria, PO Box 3065, Victoria, British Columbia, V8W 3V6, Canada
[c] Laboratorio de Química Biológica, Faculdad de Química, Pontificia Universidad Católica de Chile, Santiago, Chile
[d] Key Lab of Green Chemistry and Technology, College of Chemistry, Sichuan University, Wangjiang Road, Chengdu 610064, China

† Electronic Supplementary Information (ESI) available: [Experimental section including Instruments, Materials, and Sample Preparation, 2D-NMR analyses, UV-vis, CD, fluorescence, and excitation spectroscopies, Results of Monte-Carlo conformer search of the duplex model, and first-order kinetic plots.]. See DOI: 10.1039/x0xx00000x

We have recently shown that native Cur interacts with water-soluble cationic PT, i.e. 2,5-poly(3-(6-pyridiniohexyl)thiophene) (PyPT; Fig. 1), in an aqueous solution containing 10% DMSO to give in situ hybrid complex, which is susceptible specifically to tetrasaccharide acarbose.[7] However, the real origin of this acarbose-specific sensing by the Cur-PyPT hybrid system was not clear at that time. In this study, we examined the effects of various environmental factors on the hybridization behavior of Cur and SPG with PyPT to reveal the unprecedented melting behavior of Cur assisted by the cationic hybridization partner as well as the unexpectedly dynamic and multifaceted nature of the glucan-PT hybridization, involving the competitive hetero-duplex/triplex formation, as summarized in Scheme 1. The present results and concepts will promote the mechanistic understanding of polysaccharide hybridization in general and stimulate the development of glucan-based switchable sensing, delivery, and memory systems using environmental factors as convenient tools.

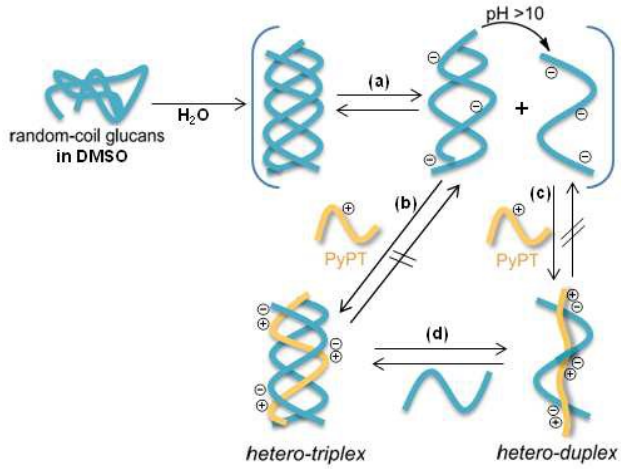

Scheme 1 Mechanism proposed for the hybridization of PyPT with Cur. (a) homo-triplex equilibrates with a pair of single- and double-stranded Cur, which is driven by partial deprotonation/protonation; (b) negatively charged Cur duplex captures cationic PyPT to form hetero-triplex; (c) negatively charged single-stranded Cur binds cationic PyPT to form loosely bound hetero-duplex; (d) hetero-triplex and duplex thus formed equilibrate with each other.

Results and discussion

1. Cur-PyPT system

UV-vis, circular dichroism, and NMR spectral examinations

Complexation behavior of the Cur-PyPT system was first examined by UV-vis and circular dichroism (CD) spectroscopies in 1:9 (v/v) DMSO/H_2O, which can solubilize native Cur in up to 1.0 mM (hereafter, all polymer concentrations are in monomer unit). As shown in Fig. 2 (black line), PyPT dissolved in 1:9 DMSO/H_2O exhibited a broad absorption band at 448 nm, assignable to the π,π^* transition, and naturally no CD signals excepting the baseline drift and the electric noises of <0.5 mdeg. An aqueous DMSO solution prepared by adding an aqueous solution of PyPT (9 parts) to a DMSO solution of Cur (1 part) showed essentially the same UV-vis spectrum as that of the pure PyPT solution, but exhibited a positive couplet at the main band of PT (Fig. 2, red line), the sign of which indicates a right-handed helical arrangement induced to the PT chromophore, according to the exciton chirality theory.[8]

Although the helicity assigned coincides with that of Cur triplex, this does not immediately help us discriminating between the two plausible mechanisms mentioned above: (1) the PT main chain is included in the hydrophobic hollow core of triple-stranded Cur, or (2) PyPT forms a hetero-triplex with Cur by replacing one of the three glucan components as was the case with the hetero-triplexes of SPG.[2a,9] Hence, we first employed amylose, a linear polysaccharide composed of (1→4)-linked α-D-glucose units, as a reference, since amylose is known to form a left-handed single helix in aqueous DMSO solution[2b-f,4b,10] and binds hydrophobic molecules in its helix interior. As shown in Fig. 2 (blue line), the addition of amylose caused a significant hypsochromic shift and sharpening of the main band in the UV-vis spectrum of PyPT, indicating shortened conjugation length and less flexible conformation. In the CD spectrum, a bisignate Cotton effect was induced upon addition of amylose, but this signal does not appear to arise from the exciton coupling interaction of the PT main band, simply because the agreement in wavelength of the negative CD extremum with the UV-vis maximum; if the bisignate signal was an exciton couplet, the crossover point would appear at the same wavelength as the UV-vis maximum.

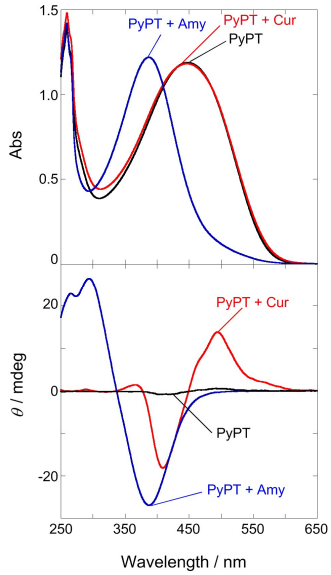

Fig. 2 UV-vis (top) and CD spectra (bottom) of PyPT (0.20 mM) in the absence (black) and presence of Cur (1.0 mM, red) and amylose (0.61 mM, blue) in a 1:9 DMSO/H_2O solution at 25 °C in a 1 cm cell.

The inclusion of PyPT by amylose was further examined by 2D NMR spectroscopy; for the original charts, see Fig. S1 in the electronic supplementary information (ESI). NOE crosspeaks occurred between the thiophene proton (H_a) of PyPT and the inner protons[2f] (H_5, H_6, and $H_{6'}$) of amylose, clearly indicating that PyPT is included in the amylose cavity. These results obtained for amylose are not compatible with the above-mentioned first mechanism that triple-stranded Cur includes PyPT in its hollow cavity, but rather support the second one that Cur forms a hetero-triplex with PyPT.

Hence, we analyzed the CD spectral titration data obtained upon addition of Cur to PyPT (0.2 mM in monomer unit) in aqueous solution containing 10% DMSO, which was reported in our previous paper,[7] to determine the hybridization stoichiometry of PyPT:Cur as 1:2. As shown in Fig. 3a, the ellipticity induced to the PyPT solution upon addition of Cur showed a saturation behavior to reach a quasi-plateau at 0.5-1.0 mM. The inflection point estimated by extrapolating the ellipticity changes in the low and high concentration regions was 0.23 mM (Fig. 3b), apparently indicating 1:1 stoichiometry (in monomer unit) for the PyPT-Cur complex; it is to note that the inflection point determined above by extrapolating the regression lines obtained by using the first two and the last three points is the upper limit, and the actual inflection concentration should be equal to or somewhat smaller than this value (0.23 mM).

Since a pair of different polymers can form a stable complex only when their hybridization unit lengths match to each other, not only the molar ratio but also the monomer unit lengths should be taken into consideration in order to determine the correct complexation stoichiometry. Thus, the monomer unit length of PyPT was estimated as 3.6 Å from the examinations of a molecular model on MM2, while that of Cur was estimated as 7.1 Å as determined in the following calculation. On the basis of the fact that the conjugation length of PyPT was significantly shortened upon complexation (see discussion below and reference 14), we consider that the PyPT main chain is in helical *syn*-conformation,[11] as was the case with the SPG/PT cohelical complex.[5f] Since the outer- and inter-diameters and the pitch of a 6_1 Cur helix are 23, 1.6, and 18 Å,[3g,4c] respectively, the mean diameter of the helix is calculated as: (23-1.6)/2 + 1.6 = 12.3 Å. Hence, the effective length of each glucose unit along the helix axis is calculated as: $[(12.3\pi)^2 + (18)^2]^{1/2}/6$ = 7.1 Å (see Fig. S2 in ESI). For a smooth hybridization, the hybridization partners should have comparable lengths and in the present case two PyPT units (7.2 Å) are matched to the length of one Cur unit (7.1 Å). If the 1:1 complexation stoichiometry is formally applied to this system, nearly half of the Cur monomer length (7.1 – 3.6 = 3.5 Å) remains uncontacted with the partner thiophene monomer, leading to a failure in forming stable hetero-complex. Thus, the apparent 1:1 stoichiometry evaluated above should be translated to the 1:2 stoichiometry, indicating formation of [PyPT•$(Cur)_2$] complex through the processes (a) and (b) in Scheme 1. Hereafter, the hybridization experiments were performed at [Cur]/[PyPT] = 5, since all of the normalized CD spectra obtained upon titration at [Cur]/[PyPT] ratio varying from 0.5 to 5 (Fig. 3a) were practically identical in shape (Fig. S3 in SI), indicating formation of [PyPT•$(Cur)_2$] complex of the same helical properties. Although such a hetero-triplex model is widely accepted,[5f,6a] the hydrogen-bonding network reconstructed in the hetero-triplex is still under investigation.

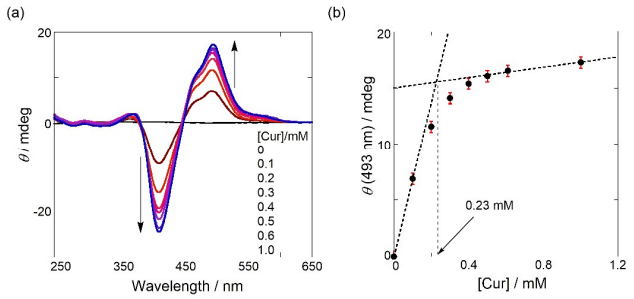

Fig. 3 (a) CD spectra of a 1:9 DMSO/H_2O solution of PyPT (0.2 mM in monomer unit) in the presence of Cur (0-1.0 mM), measured at 25 °C in a 1 cm cell. (b) Ellipticity changes at 493 nm as a function of curdlan concentration (in monomer unit).

Temperature effects

Intriguingly, the Cur-PyPT hybridization turned out to be a very slow, time-dependent process. As shown in Fig. S4 in ESI, although the UV-vis absorbance was slightly reduced with a small hypsochromic shift, the CD couplet amplitude was significantly intensified without any appreciable shape change, when the sample solution was kept still for 7 days at room temperature in the dark.

Hence, the Cur-PyPT solution was heated up to 90 °C with CD monitoring at the negative extremum (405 nm) to obtain the ellipticity change shown in Fig. 4 (black solid line). The ellipticity profile obtained looks like a melting curve of double-stranded DNA, showing a sudden change around the apparent "melting" temperature of 74 °C. However, the ellipticity was greatly enhanced from –19 to –51 mdeg upon "melting." Furthermore, upon subsequent cooling down to 25 °C, the ellipticity of the heated sample did not follow the original "melting" curve but was further augmented to –79 mdeg (Fig. 4, black dotted line), indicating occurrence of some irreversible event upon heating. The annealing process was repeated another four times (Fig. 4, pairs of solid and dotted line in different color) to afford a convergence value of –97 mdeg after the third cooling, and no practical changes were induced thereafter.

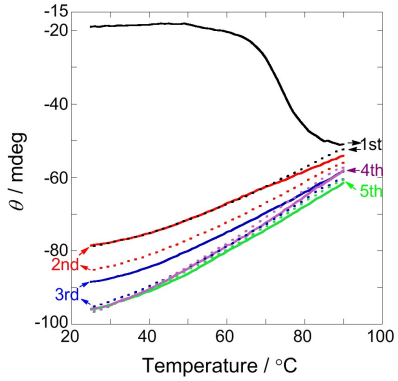

Fig. 4 Ellipticity changes monitored at 405 nm for a 1:9 DMSO/H_2O solution of PyPT (0.2 mM) and Cur (1.0 mM), measured in a 1 cm cell, upon repeated heating (solid line) and cooling (dotted line) at a heating/cooling rate of 1 °C min^{-1} for the 1st (black), 2nd (red), 3rd (blue), 4th (purple), and 5th (green) cycles; in each annealing run, the heated solution was kept at 90 °C for 30 min before subsequent cooling.

As shown in Fig. S5 in ESI, the UV-vis and CD spectral changes induced by repeated annealing were very similar to those observed upon 7-day standing at room temperature (Fig. S4 in ESI), showing appreciable hypso- and hypochromic effects in UV-vis spectrum and a significant enhancement of the couplet amplitude in CD spectrum without accompanying any essential changes in shape. These observations indicate that a single hybrid complex is formed between Cur and PyPT and the dramatic CD spectral changes observed originate from the expedited hybridization upon long-term standing at room temperature or annealing at 90 °C, rather than the reorganization of a metastable hybrid complex formed in situ upon mixing of PyPT with Cur.

These results reveal that only part of the PyPT in solution immediately hybridizes with Cur to give hetero-triplex upon addition of an aqueous solution of PyPT to a DMSO solution of random coil Cur, while most of the Cur regenerates homo-triplex (processes (a) and (b) in Scheme 1), due to the kinetic competition between the two processes. The Cur homo-triplex very slowly hybridizes with PyPT to the hetero-triplex upon long-term standing at ambient temperature (Fig. S4 in ESI), but "melts" or disassembles in the presence of PyPT to homo-duplex upon heating (>70 °C) (process (a) in Scheme 1), which immediately hybridizes with PyPT in the system to give hetero-triplex [$(Cur)_2$•PyPT] (process (b) in Scheme 1). Although a water suspension of native Cur is known to suffer significant fibrillar structural changes at 90 °C,[3c] Cur homo-triplex does not appear to dissociate in aqueous solution even at the elevated temperatures of up to 90 °C in the absence of PyPT. In contrast, SPG triple helix is known to disassemble at >135 °C in aqueous solution under sealed condition.[3f,h,i,j] Since the hybridization is greatly accelerated also at higher pH (see the next section), the dissociation of homo-triplex is thought to be triggered by the partial deprotonation of hydroxyl groups in Cur at higher temperatures,[12] indicating that the hetero-triplex thus formed is a polyionic complex in nature. The fact that neutral cyclodextrin-tethered PT does not hybridize with Cur under the comparable condition also reveals the crucial role of the cationic sidechain of PyPT in facilitating the hybridization (see Fig. S6 and the relevant discussion in ESI).

pH effects

More direct evidence for the essential role of electrostatic interactions in Cur-PyPT hybridization was obtained by the UV-vis and CD spectral examinations at higher pH. An aqueous DMSO solution prepared by adding an aqueous solution of PyPT to a DMSO solution of Cur was slightly acidic (pH 6.3) and gave the UV-vis and CD spectra shown in Fig. 5a (black line), which suffered no practical changes upon further acidification of the solution to pH 4.6 or 4.2 (Fig. 5a; turquoise and orange lines). In keen contrast, increasing the solution pH from 6.3 to 10.1 led to an enormous enhancement of the CD couplet amplitude to reach 473 mdeg at pH 10.1 (Fig. 5b) without altering the spectral shape (Fig. 5d). At pH 10.5, the couplet was appreciably red-shifted and the shoulder at 550-600 nm became more evident, which will be discussed in due order.

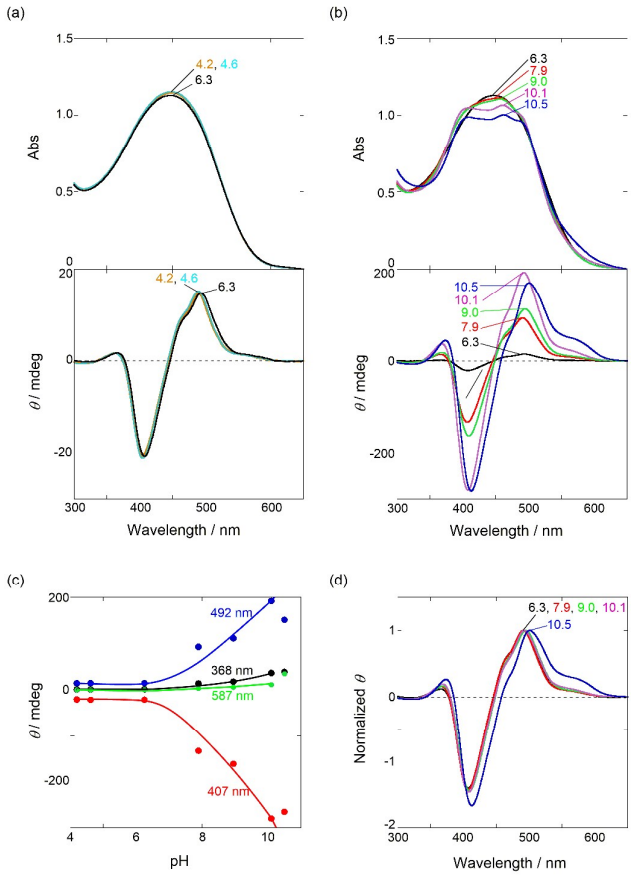

Fig. 5 (a) UV-vis and CD spectra of 1:9 DMSO/H_2O solutions of PyPT (0.2 mM) and Cur (1.0 mM) as prepared (pH 6.3, black) and acidified to pH 4.6 (turquoise), and 4.2 (orange); (b) UV-vis and CD spectra of the same solution as prepared (pH 6.3, black) and at pH 7.9 (red), 9.0 (green), 10.1 (purple), and 10.5 (blue); all measured at 25 °C in a 1 cm cell; (c) Plots of the ellipticities at 368 nm (black), 407 nm (red), 492 nm (blue), and 587 nm (green); (d) Normalized CD spectra at pH 6.3 (black), 7.9 (red), 9.0 (green), 10.1 (purple), and 10.5 (blue); the first four spectra are almost superimposable with each other.

The rapid increase of ellipticity at higher pH (of up to 10.1) is reasonably accounted for in terms of the following hybridization scenario (Scheme 1): (1) Cur homo-triplex is partially deprotonated under the basic conditions,[3l] (2) the negatively charged triplex thus formed is disassembled to a pair of single- and double-stranded Cur, and (3) the negatively charged Cur duplex captures cationic PyPT to form a polyionic complex (hetero-triplex) through electrostatic interactions to complete the hybridization. The fact that the CD spectral shape is kept unchanged over the wide pH range of 4.2-10.1 and only the amplitude is augmented in the basic solutions indicates that a single chromophoric hybrid species of exactly the same helical sense and pitch (conjugation length) exists throughout the pH range and its abundance increases with increasing pH. This allows us to estimate the fraction of PyPT incorporated in the hetero-triplex as 7-8% at pH 4.2-6.3, 48% at pH 7.9, and 58% at pH 9.0, by assuming that all PyPT in the solution forms triplex at pH 10.1. This result also reveals that the selective sensing of acarbose among several mono- to pentaoses upon hybridization of Cur with PyPT reported in our previous paper[7] was achieved not by the preferential co-hybridization (against our previous claim) but in reality by the

facilitated Cur-PyPT hybridization upon addition of basic amino saccharide acarbose.

In contrast to the highly consistent CD spectral shapes at pH 6.3-10.1 (Fig. 5d), the corresponding UV-vis spectra significantly varied in shape, gradually developing split peaks at higher pH (Fig. 5b, upper panel). This contrasting behavior of UV-vis versus CD is rather anticipated, as the majority of PyPT is free and CD-silent in acidic and less basic solutions, and hence dominates the UV-vis spectrum but never contributes to the CD spectrum. Thus, the CD couplet amplitude and the UV-vis splitting maximize at pH 10.1, where the majority of PyPT forms hetero-triplex with Cur. Since analogous splitting has been reported for several chirally modified PTs upon aggregation in poor solvents and in thin films,[13] we examined the concentration effects on the UV-vis and CD spectra of a basic Cur-PyPT solution at pH 11. However, the UV-vis and CD spectra did not show any appreciable changes in shape upon 5-fold dilution to afford essentially the same anisotropy profile (Fig. S7 in ESI). This suggests that the split UV-vis and bisignate CD signals originate from the intramolecular exciton coupling of the π,π^* transitions of adjacent oligothiophene segments[14] in the PyPT backbone conformationally fixed upon hybridization with Cur. This assignment is compatible with the observation that the UV-vis and CD extrema appear at the same wavelengths, i.e. 492, 460, and 407 nm (Fig. 5b, purple line at pH 10.1).

Intriguingly, a small increase of pH from 10.1 to 10.5 caused sudden bathochromic shifts with appreciable hypochromic effects in UV-vis and CD spectra (Figs. 5b,d), implying formation of a new chiral PyPT species that absorbs at longer wavelengths. Upon further increase of the solution pH to 11.6 and then to 12.1, the split UV-vis peaks were merged to give a smaller broad one at longer wavelengths, and the CD couplet was also reduced in intensity and greatly red-shifted without accompanying any isosbestic or isodichroic point, as shown in Fig. S8 in ESI. Since some orange material started to precipitate at pH 11.6, the reduced intensities are reasonably attributed to partial precipitation of the PyPT species formed at high pH. Nevertheless, the new PyPT species was moderately soluble in the highly alkaline solution and showed significantly red-shifted UV-vis peak and CD couplet. These spectral features are interpreted only by the formation of Cur-PyPT hetero-duplex that possesses a longer conjugation length and a looser helix of the same chiral sense as the hetero-triplex. In this relation, Shinkai et al. reported that per-6-PEGylated Cur binds a water-soluble cationic PT to form a loose hetero-duplex, which also exhibits a positive exciton couplet at 400-600 nm.[6a] A 1:9 DMSO/H_2O solution of PyPT and Cur at pH 6.3 also showed a less intense positive Cotton effect at 550-600 nm (Fig. 5d), indicating formation of a small amount of Cur-PyPT hetero-duplex. This result reveals that the negatively charged single-stranded Cur formed in process (a) hybridizes with PyPT to give a hetero-duplex at less basic and even slightly acidic pH (process (c)). The hetero-triplex and hetero-duplex formed in processes (b) and (c) are highly stabilized as polyionic complexes and the hybridizations are practically irreversible.

Zeta potential

To further confirm the formation of polyionic complexes, we measured the zeta (ζ) potential of the hetero-triplex and hetero-duplex. The ζ values of PyPT (0.2 mM) and Cur (1.0 mM) in aqueous solution containing 10% DMSO were determined as +40.4 and +0.1 mV, respectively, indicating that PyPT and Cur are respectively a cationic and a neutral polymer. When PyPT (0.2 mM) was mixed with Cur (1.0 mM) at pH 6.3 (the condition for hetero-triplex formation), the ζ potential decreased to +6.5 mV, clearly indicating that the cationic PyPT was significantly neutralized by deprotonated anionic Cur and thus the hetero-triplex is polyionic in nature. Furthermore, the ζ value of a solution of PyPT (0.2 mM) and Cur (1.0 mM) at pH 12.1 (the condition for hetero-duplex formation) was inverted in sign to -2.1 mV and therefore further deprotonated Cur hybridizes with cationic PyPT to form a hetero-duplex.

Monte-Carlo simulation of hetero-duplex

Since the positive Cotton effect observed at 550-600 nm was assigned to the hetero-duplex, the ellipticity changes at 580 nm obtained upon CD spectral titration of 0.2 mM PyPT with Cur at pH 6.3 (Fig. 3a) was plotted against the Cur concentration. As shown in Fig. 6a, an inflection point was observed at [Cur] = 0.61 mM, suggesting the 1:3 stoichiometry. This is however an apparent value (as was the case with the hetero-triplex discussed above), and the real stoichiometry should be calculated by taking into account the relative helical pitch of the hybridization partners in hetero-duplex.

Since no plausible hetero-duplex model supported by theory has been proposed for Cur and cationic PT, we decided to elucidate the structure of the hetero-duplex of Cur with PyPT by the Monte-Carlo conformer search of MacroModel 10.6 module.[15] Judging from the much longer conjugation length of ≥20 thiophene units[14] (as indicated by the main band appeared at 461 nm) than that (9 thiophene units) of hetero-triplex, in which PT is in helical *syn*-conformation,[11] we postulated that PyPT in hetero-duplex adopts the helical *anti*-conformation.[11]

As an initial structure of the hetero-duplex model for the Monte-Carlo conformer search, we employed *anti*-3,4',4'',4''',4'''',4'''''-hexakis(6-pyridiniohexyl)-2,2':5',2'':5'',2''':5''',2'''':5'''',2''''':5''''',2'''''-sexithiophene (6-mer, PyST), which was prepared by connecting three units of *anti*-3,4'-bis(6-pyridiniohexyl)-2,2'-bithiophene (2-mer, PyBT) pre-optimized by the Hartree-Fock calculation, and a single-stranded glucose 18-mer, which was constructed by connecting three 6-mer units sliced out from the crystal structure of triple-stranded Cur[3g] and subsequent adjusting to the length of PyST (see Fig. S9 in ESI and the relevant discussion). Figs. 6b and 6c show the second-stable structure, in which the negatively-charged glucose 18-mer nicely fits to the PyST unit in length, forming a loose duplex, while the glucose 18-mer in the most stable structure (Fig. S9 in ESI) was more extended, which may hinder hybridization of polymeric Cur with PyPT, and hence is not valid.

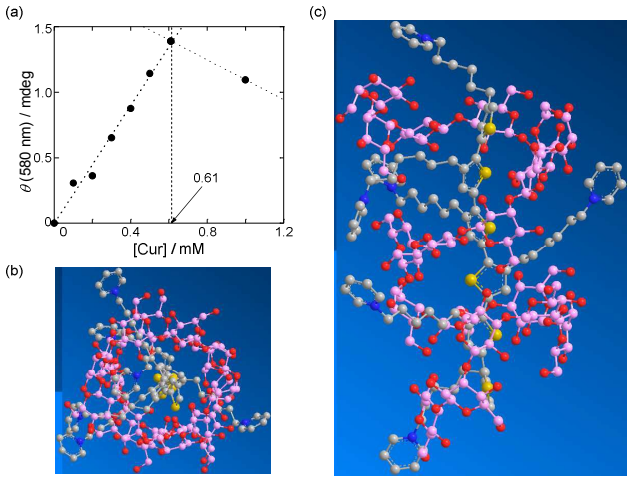

Fig. 6 (a) Ellipticity changes at 580 nm as a function of [Cur]; see Fig. 3a for the original titration data. (b) Top and (c) front views of the structure of the second-stable hetero-duplex model, composed of PyST 6-mer and glucose 18-mer, which was obtained by geometry-optimization by the Monte-Carlo conformer search using the OPLS-2005/H_2O force field (1000 steps). Hydrogen atoms in the hetero-duplex model were omitted for clarity.

Most of the essential processes shown in Scheme 1 are now experimentally and/or theoretically supported. Thus, upon addition of an aqueous solution of PyPT to a DMSO solution of random-coil Cur, most of the Cur forms homo-triplex and only part of PyPT hybridizes in situ with Cur to give hetero-triplex [PyPT•$(Cur)_2$], where the interconversion between homo- and hetero-triplex appears to be extremely slow at least at room temperature. As the hetero-triplex is polyionic in nature, the hybridization is greatly promoted by raising the solution pH to 7-10 or the temperature to >70 °C, both of which facilitate deprotonation of the hydroxyl groups in Cur and the subsequent dissociation to negatively charged Cur duplex, which is immediately captured by cationic PyPT to form polyionic Cur-PyPT hetero-triplex. At pH ≥10.5, further deprotonation from Cur in the hetero-triplex leads to dissociation to single-strand Cur and polyionic hetero-duplex [PyPT•Cur], the latter of which is looser in conformation and longer in conjugation length, but possesses the same helical sense as the hetero-triplex. The equilibrium between hetero-triplex and hetero-duplex, i.e. process (d) in Scheme 1, will be discussed in the next section.

Hetero-triplex/duplex equilibrium

The equilibrium between hetero-triplex and hetero-duplex was investigated with a Cur-PyPT solution at pH 10.5, where the hetero-triplex is already dissociated at least in part to the hetero-duplex (Fig. 5d and the relevant discussion) and is expected to further dissociate at elevated temperatures. The Cur-PyPT solution at 25 °C was heated to 90 °C (at a rate of 1 °C min^{-1}) and then kept at that temperature for 5 h with UV-vis and CD spectral monitoring. As shown in Fig. 7a (compare the black line with the red line), the initial heating caused a growth of new UV-vis and CD bands at 530-630 nm at the expense of the original intensity at shorter wavelengths, indicating dissociation of the hetero-triplex to a looser hetero-duplex. Somewhat unexpectedly, the subsequent standing at 90 °C induced gradual hypsochromic shifts of the UV-vis and CD spectra with an isosbestic point at 431 nm and isodichroic points at 431 and 528 nm; see the spectral changes from the red to blue lines in Fig. 7a, slowly regenerating the original spectra of hetero-triplex. These apparently strange sequential UV-vis and CD spectral changes are rationalized by assuming that the Cur incorporated in a hetero-triplex deprotonates at higher temperatures to develop negative charges on the triplex, the subsequent dissociation of which is facilitated by the spontaneous hydration to both of the hetero-duplex and single-stranded Cur thus generated. However, the hydrated duplex-Cur pair is thermodynamically less stable and reassembles to a hetero-triplex but only at a very slow rate (taking hours) due to the slow dehydration dynamics. Similar slow dehydration dynamics has been reported for DNA films and cyclodextrin microcrystals in the air.[16]

According to the above mechanism, the reassembling rate constant (k_a) at 90 °C was evaluated as 1.5 x 10^{-4} s^{-1} from the pseudo-first order kinetics plot of the ellipticity changes monitored at 610 nm (Fig. S10b in ESI). The pseudo-first order kinetics observed is rationalized by assuming that an excess amount of single-strand Cur generated from the dissociation of hetero-triplex as well as homo-triplex upon heating is available in the basic solution. Similar treatments of the ellipticity changes at 85 °C and 95 °C gave the k_a values of 1.1 x 10^{-4} and 1.9 x 10^{-4} s^{-1}, respectively (Figs. S10a and S10c in ESI). These rate constants were subjected to the Eyring analysis to give a straight line shown in Fig. 7b, from which the activation parameters for the reassembling of hetero-duplex to hetero-triplex were evaluated: $\Delta H^{\ddagger}$ = 60 ± 2 kJ mol^{-1} and $\Delta S^{\ddagger}$ = 91 ± 6 J K^{-1} mol^{-1}. The positive activation enthalpy and entropy are reasonable for the association process that involves the release of multiple water molecules; i.e. the process (d) in Scheme 1.

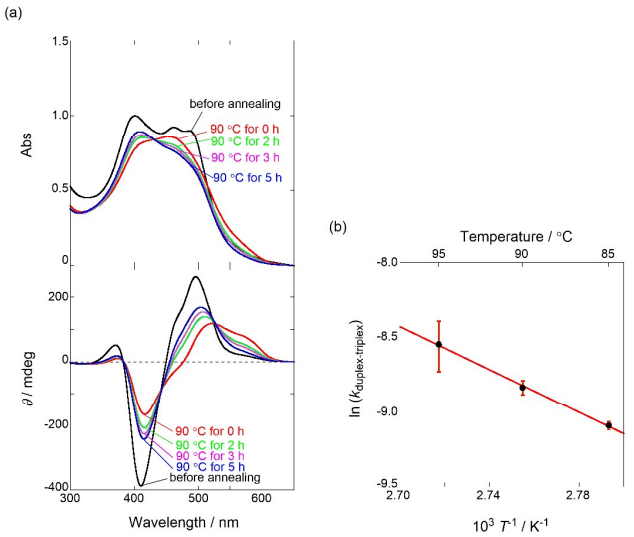

Fig. 7 (a) UV-vis (top) and CD (bottom) spectra of a 1:9 DMSO/H_2O solution (pH 10.5) of PyPT (0.2 mM) and Cur (1.0 mM) in a 1 cm cell at 25 °C before annealing (black) and at 90 °C after annealing, holding for 0 h (red), 2 h (green), 3 h (purple) and 5 h (blue); PyPT was totally stable under the condition employed. (b) Eyring plot of the rate constants (k_a) for the reassembling of Cur-PyPT hetero-duplex to hetero-triplex in a DMSO-H_2O (1:9) solution.

Salt effects

Given that the major driving force for the Cur-PyPT hybridization is the electrostatic interaction as elucidated above, the hybridization behavior is expected to be affected by the addition of electrolytes. To confirm this, we examined the salt effects on the UV-vis and CD spectra of a Cur-PyPT solution at pH 10.1, which contained the hetero-triplex as the dominant species. As shown in Fig. S11 in ESI, both of the UV-vis and CD spectra were gradually red-shifted with accompanying isosbestic/isodichroic points upon addition of NaCl in 1-4 M or even higher concentrations. The spectral changes induced are very similar to those observed upon heating up to 90 °C (Fig. 7a), indicating dissociation of hetero-triplex to hetero-duplex and Cur (process (d)) at high salt concentrations or elevated temperatures facilitated by weakening the electrostatic interactions in polyionic complex or by accelerating the deprotonation of Cur's hydroxyl group, respectively.

Fluorescence spectral examinations

PT is known to weakly fluoresce in aqueous solution,[17] which allowed us to examine and compare the excited-state behaviors of free and hybridized PyPT. The results of fluorescence spectral examinations and the relevant discussion (presented in Figs. S12-14 of ESI) provided further evidence in support of the hybridization mechanism proposed in Scheme 1.

NMR DOSY spectral and dynamic light scattering examinations

To gain the size information for the species formed upon hybridization, we examined the hybridization behavior by using 2D-DOSY and dynamic light scattering (DLS) methods. The DOSY spectra obtained for PyPT and its mixture with Cur in 3:7 DMSO-d_6/D_2O suffered significant peak broadening and were not suitable for reliable analysis (Fig. S15 in ESI), while the DLS measurements for a PyPT-Cur mixture (0.2 and 1.0 mM, respectively) in 1:9 DMSO/H_2O gave a broad peak at hydrodynamic diameter (d_h) of 2.3 μm at pH 6.3 and of 2.1 μm at pH 12.1, which are tentatively assigned to the hetero-triplex and hetero-duplex, respectively.

The length of a fully extended triplex of Cur 8018-mer (1300 kDa) employed in this study is estimated as 2.4 μm from the pitch of Cur 6_1 triplex (1.8 nm) in crystal.[3g,4c] This cylindrical Cur homo-triplex of 2.3 nm diameter[3g,4c] is equivalent in volume to a sphere of 27 nm diameter, which is however much smaller than the d_h values (2.1-2.3 μm) obtained by the DLS measurements mentioned above, suggesting formation of some aggregates. Hence, we examined the concentration effects on the d_h value by diluting the PyPT/Cur solutions by a factor of 5, 10, and 20 to observe a sudden decrease of d_h from 2.3 μm to 62 nm upon 5-fold dilution and to consistent 34 nm, a reasonable size for a single hetero-triplex, upon 10- and 20-fold dilutions for the hetero-triplex at pH 6.3, but a much slower decrease of d_h from 2.1 μm to 2.0 μm upon 5-fold dilution and to 480 and 140 nm upon 10- and 20-fold dilutions for the hetero-duplex at pH 12.1, as shown in Fig. 8; further dilution was not feasible due to the weak DLS signals. These results reveal that the aggregation behavior greatly differs between the hetero-triplex and the hetero-duplex, the latter of which much more easily aggregates even in a solution of 0.01 mM PyPT and 0.05 mM Cur. This seems reasonable, as the hetero-duplex generated at pH 12.1, possessing a ζ potential of –2.1 mV, is more charge-neutralized than the hetero-triplex with a ζ potential of +6.5 mV. The concentration effect is discussed in further detail in ESI (Fig. S16 and the relevant discussion).

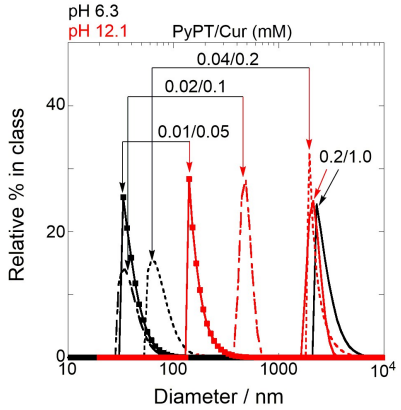

Fig. 8 DLS examinations of 1:9 DMSO-H_2O solutions of PyPT and Cur at 0.2 and 1.0 mM (solid line), 0.04 and 0.2 mM (dotted line), 0.02 and 0.1 mM (dashed line), and 0.01 and 0.05 mM concentrations (square-marked solid line) at pH 6.3 (black) and 12.1 (red) at 25 °C.

2. SPG-PyPT complexation

UV-vis and CD spectral examinations

Learning that the hybridization of PyPT with Cur is greatly accelerated by the deprotonation of the latter at elevated temperatures and pH to form a polyionic hybrid complex, we explored the scope of this novel hybridization mechanism by using schizophyllan (SPG). SPG differs from Cur in branching and chain length (molecular weight = 1.30 x 10^6 for Cur and 1.44 x 10^5 for SPG) (Fig. 1), but forms homo-triplex that similarly behaves to denature in DMSO and renature in aqueous solution.

We first employed neutral CDPT (Fig. S6a in ESI) as a hybridization partner, which however showed no induced Cotton effects upon mixing with SPG (Fig. S17 in ESI), indicating that the non-charged PT does not appreciably hybridize with SPG at least at 25 °C, as is the case with Cur. This result reconfirms that the hydrophobic interaction between CDPT and SPG is not sufficient to form a hetero-triplex.

In sharp contrast, addition of an aqueous solution of PyPT to a DMSO solution of SPG induced a major splitting of the π,π* transition of PyPT in the UV-vis spectrum and a strong positive couplet (crossover point at 445 nm) of an amplitude as large as 640 mdeg, which was accompanied by a positive peak (shoulder) at 550-600 nm, in the CD spectrum (Fig. 9a, black line). Acidification of the solution down to pH 4.9 (red line) further intensified the couplet amplitude up to 788 mdeg at the expense of the positive peak at longer wavelengths. The immediate development of the intense exciton couplet even at

pH 6.5 is attributable to the higher solubility of SPG than that of Cur in water, which facilitates rapid hybridization upon mixing with PyPT.

Upon gradual increase of the solution pH from 6.5 to 14.0, the original strong CD couplet faded out to give an equally intense positive couplet (crossover point at 506 nm) at longer wavelengths with accompanying quasi-isodichroic points at 443 nm and 524 nm, while the split UV-vis absorption globally moved to longer wavelengths, as shown in Fig. 9b. These CD and UV-vis spectral behaviors are very similar to those observed for the Cur-PyPT system (Fig. 5) and hence reasonably assignable to the disassembling of polyionic SPG-PyPT hetero-triplex to hetero-duplex driven by the deprotonation of SPG facilitated at higher pH. It is to note that the CD spectra of Cur-PyPT and SPG-PyPT triplexes closely resemble to each other in shape and transition energy (Figs. 5b and 9a), indicating that nearly the same helical conformation of PyPT is achieved in the two triplexes. In contrast, the CD spectra of the corresponding duplexes differ in shape and crossover wavelength; compare Figs. S8 in ESI (blue line) and 9b (orange line). The crossover occurs at 532 nm for Cur but at 513 nm for SPG, suggesting shorter conjugation length and hence a tighter duplex structure for the latter, presumably due to the sidechain. It is to note that the present hybridization mechanism (Scheme 1) is applicable not only to unbranched glucan Cur but also to branched glucan SPG, and also that the CD spectroscopy is the most convenient and efficient tool for tracking the dynamic hybridization processes to hetero-triplex and hetero-duplex.

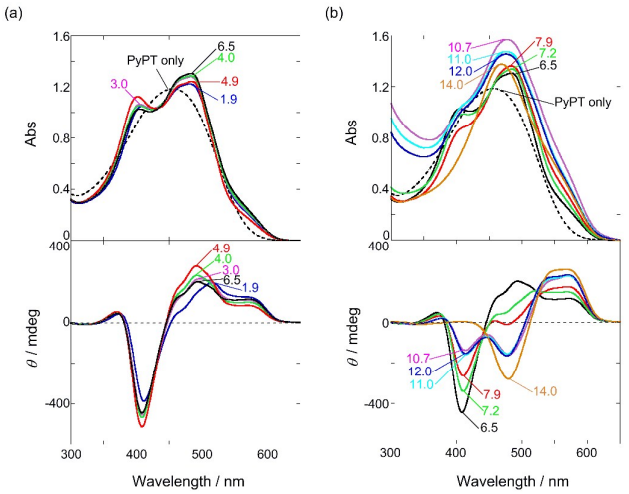

Fig. 9 (a) UV-vis and CD spectra of 1:9 DMSO/H_2O solutions of PyPT (0.2 mM) and SPG (1.0 mM) at pH 1.9 (blue), 3.0 (purple), 4.0 (green), 4.9 (red), and 6.5 (black) and (b) UV-vis and CD spectra of the same solution at pH 6.5 (black), 7.2 (green), 7.9 (red), 10.7 (purple), 11.0 (light blue), 12.0 (blue), and 14.0 (orange); the UV-vis spectrum (dotted black line) of PyPT in DMSO-H_2O (1:9); all spectra recorded at 25 °C in a 1 cm cell.

Conclusions

In the present study, we have elucidated the mechanism of dynamic glucan-polythiophene hybridization by using curdlan and schizophyllan as representative unbranched and branched linear polysaccharides and polycationic PyPT as a chromophoric hybridization partner. The in situ hybridization to hetero-triplex [$(Cur)_2$•PyPT] upon addition of an aqueous solution of PyPT to a DMSO solution of Cur at ambient temperatures turned out to be far from completion (processes (a) and (b) in Scheme 1). Indeed, the hybridization was greatly accelerated by raising the solution temperature or pH to reach a saturation at 90 °C or at pH 10.5, indicating that the hybridization is driven by the partial deprotonation and subsequent disassembling of Cur homo-triplex to negatively charged homo-duplex (process (a)), which spontaneously hybridizes with positively charged PyPT to give a polyionic hetero-triplex (major (b) and minor (c)). It should be emphasized that *polycationic PyPT can unzip Cur homo-triplex and hybridize with the resulting homo-duplex in neutral aqueous solutions*, despite that Cur homo-triplex does not show any sign of disassembling even at high temperatures in the absence of PyPT or in the presence of neutral PT. Interestingly, the hetero-triplex disassembles to hetero-duplex at very high pH (>11) through further deprotonation from Cur in the hetero-triplex (process (d)). Since SPG hybridizes similarly or even more readily with PyPT, this hybridization mechanism (Scheme 1) should operate more generally with any combinations of glucans and cationic polymers to find applications in stimulus-responding molecular and chirality sensing and delivery systems and switchable memory applications, and ultimately chiral supramolecular architecture construction.

Acknowledgements

We thank Mitsui Sugar Co., Japan, for providing schizophyllan, Dr. Yuichiro Hori and Prof. Kazuya Kikuchi of Osaka University for the use of the MacroModel software, and Prof. Munenori Numata of Kyoto Prefectural University for the fruitful discussion. This work was supported by Grant-in-Aid for Young Scientists (B) (No. 23750129), Challenging Exploratory Research (No. 26620061), and Young Scientists (A) (No. 16H06041) for GF and Grant-in-Aid for Scientific Research (A) (No. 21245011) and Challenging Exploratory Research (No. 26620030) for YI, all from Japan Society for the Promotion of Science (JSPS), and also by the grants for GF from The Ogasawara Foundation for the Promotion of Science & Engineering and Nakatani Foundation. CB thanks the Natural Sciences and Engineering Research Council of Canada (NSERC) for financial support in the form of a Discovery Grant. CY thanks the National Natural Science Foundation of China for financial support (No. 21372165 and 23321061).

Notes and references

1 For representative reviews, see: (a) J. J. L. M. Cornelissen, A. E. Rowan, R. J. M. Nolte and N. A. J. M. Sommerdijk, *Chem. Rev.*, 2001, **101**, 4039; (b) M. J. Frampton and H. L. Anderson, *Angew. Chem., Int. Ed.*, 2007, **46**, 1028; (c) S. W. Thomas III, G. D. Joly and T. M. Swager, *Chem. Rev.*, 2007, **107**, 1339; (d) K. Sada, M. Takeuchi, N. Fujita, M. Numata and S. Shinkai, *Chem. Soc. Rev.*, 2007, **36**, 415; (e) T. F. A. De Greef, M. M. J.

Smulders, M. Wolffs, A. P. H. J. Schenning, R. P. Sijbesma and E. W. Meijer, *Chem. Rev.*, 2009, **109**, 5687; (f) M. M. Caruso, D. A. Davis, Q. Shen, S. A. Odom, N. R. Sottos, S. R. White and J. S. Moore, *Chem. Rev.*, 2009, **109**, 5755; (g) E. Yashima, K. Maeda, H. Iida, Y. Furusho and K. Nagai, *Chem. Rev.*, 2009, **109**, 6102; (h) B. M. Rosen, C. J. Wilson, D. A. Wilson, M. Peterca, M. R. Imam and V. Percec, *Chem. Rev.*, 2009, **109**, 6275; (i) G. R. Bhimanapati, Z. Lin, V. Meunier, Y. Jung, J. Cha, S. Das, D. Xiao, Y. Son, M. S. Strano, V. R. Cooper, L. Liang, S. G. Louie, E. Ringe, W. Zhou, S. S. Kim, R. R. Naik, B. G. Sumpter, H. Terrones, F. Xia, Y. Wang, J. Zhu, D. Akinwande, N. Alem, J. A. Schuller, R. E. Schaak, M. Terrones and J. A. Robinson, *ACS Nano*, 2015, **9**, 11509.

2 For recent representative papers and reviews, see: (a) K. Sakurai and S. Shinkai, *J. Am. Chem. Soc.*, 2000, **122**, 4520; (b) A. Star, D. W. Steuerman, J. R. Heath and J. F. Stoddart, *Angew. Chem., Int. Ed.*, 2002, **41**, 2508; (c) T. Sanji, N. Kato and M. Tanaka, *Org. Lett.*, 2006, **8**, 235; (d) M. Ikeda, Y. Frusho, K. Okoshi, S. Tanahara, K. Maeda, S. Nishino, T. Mori and E. Yashima, *Angew. Chem., Int. Ed.*, 2006, **45**, 6491; (e) O.-K. Kim, J. Melinger, S.-J. Chung and M. Pepitone, *Org. Lett.*, 2008, **10**, 1625; (f) M. J. Frampton, T. D. W. Claridge, G. Latini, S. Brovelli, F. Cacialli and H. L. Anderson, *Chem. Commun.*, 2008, 2797; (g) G. K. Such, A. P. R. Johnston and F. Caruso, *Chem. Soc. Rev.*, 2011, **40**, 19; (h) X. Li, Y. Gao and M. J. Serpe, *Macromol. Rapid Commun.*, 2015, **36**, 1382 and references therein.

3 (a) K. Ogawa, T. Watanabe, J. Tsurugi and S. Ono, *Carbohydr. Res.*, 1972, **23**, 399; (b) K. Ogawa, M. Miyagi, T. Fukumoto and T. Watanabe, *Chem. Lett.*, 1973, 943; (c) T. Harada, A. Koreeda, S. Sato and N. Kasai, *J. Electron Microsc.*, 1979, **28**, 147; (d) T. Yanaki, T. Norisuye and H. Fujita, *Macromolecules,* 1980, **13**, 1462; (e) Y. Deslandes, R. H. Marchessault and A. Sarko, *Macromolecules,* 1980, **13**, 1466; (f) T. Sato, T. Norisuye and H. Fujita, *Carbohydr. Res.*, 1981, **95**, 195; (g) C. T. Chuah, A. Sarko, Y. Deslandes and R. H. Marchessault, *Macromolecules,* 1983, **16**, 1375; (h) T. Yanaki, K. Tabata and T. Kojima, *Carbohydr. Polym.*, 1985, **5**, 275; (i) S. Kitamura and T. Kuge, *Biopolym.*, 1989, **28**, 639; (j) B. T. Stokke, A. Elgsaeter, D. A. Brant and S. Kitamura, *Macromolecules,* 1991, **24**, 6349; (k) S. Kitamura, T. Hirano, K. Takeo, H. Fukada, K. Takahashi, B. H. Falch and B. T. Stokke, *Biopolym.*, 1996, **39**, 407; (l) L. Zhang, C. Wang, S. Cui, Z. Wang and X. Zhang, *Nano Lett.*, 2003, **3**, 1119.

4 For reviews, see: (a) K. Sakurai, K. Uezu, M. Numata, T. Hasegawa, C. Li, K. Kaneko and S. Shinkai, *Chem. Commun.*, 2005, 4383; (b) M. Numata and S. Shinkai, *Adv. Polym. Sci.*, 2008, **220**, 65; (c) M. Numata and S. Shinkai, *Chem. Commun.*, 2011, **47**, 1961; (d) Y. Zhang, H. Kong, Y. Fang, K. Nishinari and G. O. Phillips, *Bioact. Carbohydr. Diet. Fibr.*, 2013, **1**, 53.

5 (a) C. Li, M. Numata, A.-H. Bae, K. Sakurai and S. Shinkai, *J. Am. Chem. Soc.*, 2005, **127**, 4548; (b) C. Li, M. Numata, T. Hasegawa, K. Sakurai and S. Shinkai, *Chem. Lett.*, 2005, **34**, 1354; (c) C. Li, M. Numata, T. Hasegawa, T. Fujisawa, S. Haraguchi, K. Sakurai and S. Shinkai, *Chem. Lett.*, 2005, **34**, 1532; (d) S. Haraguchi, M. Numata, C. Li, Y. Nakano, M. Fujiki and S. Shinkai, *Chem. Lett.*, 2009, **38**, 254; (e) S. Haraguchi, Y. Tsuchiya, T. Shiraki, K. Sada and S. Shinkai, *Chem. Commun.*, 2009, 6086; (f) S. Haraguchi, Y. Tsuchiya, T. Shiraki, K. Sugikawa, K. Sada and S. Shinkai, *Chem. Eur. J.*, 2009, **15**, 11221.

6 (a) T. Shiraki, A. Dawn, Y. Tsuchiya and S. Shinkai, *J. Am. Chem. Soc.*, 2010, **132**, 13928; (b) L. T. N. Lien, T. Shiraki, A. Dawn, Y. Tsuchiya, D. Tokunaga, S. Tamura, N. Enomoto, J. Hojo and S. Shinkai, *Org. Biomol. Chem.*, 2011, **9**, 4266; (c) M. Numata, D. Kinoshita, N. Hirose, T. Kozawa, H. Tamiaki, Y. Kikkawa and M. Kanesato, *Chem. Eur. J.*, 2013, **19**, 1592; (d) S. Tamaru, K. Hori and S. Shinkai, *Chem. Lett.*, 2015, **44**, 1667.

7 G. Fukuhara and Y. Inoue, *J. Am. Chem. Soc.*, 2011, **133**, 768.

8 (a) N. Harada and K. Nakanishi, *Circular Dichroic Spectroscopy–Exciton Coupling in Organic Stereochemistry*, University Science Books, Mill Valley, CA, 1983; (b) N. Berova, L. D. Bari and G. Pescitelli, *Chem. Soc. Rev.*, 2007, **36**, 914.

9 (a) T. Kimura, K. Koumoto, K. Sakurai and S. Shinkai, *Chem. Lett.*, 2000, 1242; (b) M. Numata, T. Matsumoto, M. Umeda, K. Koumoto, K. Sakurai and S. Shinkai, *Bioorg. Chem.*, 2003, **31**, 163; (c) T. Hasegawa, M. Umeda, T. Matsumoto, M. Numata, M. Mizu, K. Koumoto, K. Sakurai and S. Shinkai, *Chem. Commun.*, 2004, 382; (d) T. Hasegawa, T. Fujisawa, M. Numata, T. Matsumoto, M. Umeda, R. Karinaga, M. Mizu, K. Koumoto, T. Kimura, S. Okumura, K. Sakurai and S. Shinkai, *Org. Biomol. Chem.*, 2004, **2**, 3091; (e) T. Hasegawa, T. Fujisawa, S. Haraguchi, M. Numata, R. Karinaga, T. Kimura, S. Okumura, K. Sakurai and S. Shinkai, *Bioorg. Med. Chem. Lett.*, 2005, **15**, 327; (f) T. Shiraki, Y. Tsuchiya, T. Noguchi, S. Tamaru, N. Suzuki, M. Taguchi, M. Fujiki and S. Shinkai, *Chem. Asian J.*, 2014, **9**, 218.

10 G. Fukuhara, T. Nakamura, C. Yang, T. Mori and Y. Inoue, *Org. Lett.*, 2010, **12**, 3510.

11 C. X. Cui and M. Kertesz, *Phys. Rev. B,* 1989, **40**, 9661.

12 Although no literature data was available for the pK_a value of Cur, the glucose's 2-OH of α- to γ-cyclodextrins are known to be relatively acidic as aliphatic OH (pK_a = 12.33, 12.20, and 12.08, respectively); W. Saenger, J. Jacob, K. Gessler, T. Steiner, D. Hoffmann, H. Sanbe, K. Koizumi, S. M. Smith and T. Takaha, *Chem. Rev.,* 1998, **98**, 1787; B. Gillet, D. J. Nicole and J.-J. Delpuech, *Tetrahedron Lett.*, 1982, **23**, 65. It seems reasonable therefore to assume that the secondary OH of Cur is similarly acidic and the acidity is enhanced at higher temperatures to facilitate the hybridization with PyPT. Indeed, the acidity of aromatic alcohols is known to increase at higher temperatures; F. Rived, M. Rosés and E. Bosch, *Anal. Chimica Acta,* 1998, **374**, 309.

13 (a) B. M. W. Langeveld-Voss, R. A. J. Janssen, M. P. T. Christiaans, S. C. J. Meskers, H. P. J. M. Dekkers and E. W. Meijer, *J. Am. Chem. Soc.*, 1996, **118**, 4908; (b) B. M. W. Langeveld-Voss, M. P. T. Christiaans, R. A. J. Janssen and E. W. Meijer, *Macromolecules,* 1998, **31**, 6702; (c) B. M. W. Langeveld-Voss, R. A. J. Janssen and E. W. Meijer, *J. Mol. Struc.*, 2000, **521**, 285; (d) Z.-B. Zhang, M. Fujiki, M. Motonaga, H. Nakashima, K. Torimitsu and H.-Z. Tang, *Macromolecules,* 2002, **35**, 941; (e) H. Goto, Y. Okamoto and E. Yashima, *Macromolecules,* 2002, **35**, 4590; (f) C. R. G. Grenier, S. J. George, T. J. Joncheray, E. W. Meijer and J. R. Reynolds, *J. Am. Chem. Soc.*, 2007, **129**, 10694.

14 The π,π^* transition energy of PT is known to saturate at 461 nm for ≥20 mers in tetrahydrofuran; N. Sumi, H. Nakanishi, S. Ueno, K. Takimiya, Y. Aso and T. Otsubo, *Bull. Chem. Soc. Jpn.*, 2001, **74**, 979. In our case measured in 1:9 DMSO/H_2O, the π,π^* transition of free PyPT (113mer) appeared at 448 nm but was blue-shifted by 13 nm to 435 nm upon complexation with Cur, indicating that the effective conjugation length of PyPT is reduced to 9 mer in the hetero-triplex and ≥20 mer in the hetero-duplex on the basis of the estimation from the linear relationship of the conjugation length with the transition energy.

15 MacroModel, version 10.6, Schrödinger, LLC, New York, NY, 2014.

16 (a) A. Moreira da Silva, T. Steiner, W. Saenger, J. Empis and J. J. C. Teixeira-Dias, *Chem. Commun.*, 1996, 1871; (b) C. Kistner, A. André, T. Fischer, A. Thoma, C. Janke, A. Bartels, T. Gisler, G. Maret and T. Dekorsy, *Appl. Phys. Lett.*, 2007, **90**, 233902.

17 G. Fukuhara and Y. Inoue, *Chem*. *Eur*. *J*., 2012, **18**, 11459.

Table of Contents

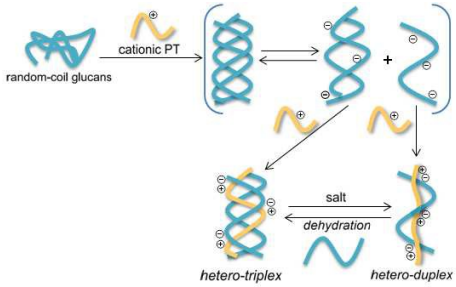

A hetero-triplex composed of a glucan and a cationic polythiophene was dynamic and disassembled to hetero-duplex in basic solutions.